Organic & Biomolecular Chemistry

Cite this: *Org. Biomol. Chem.*, 2012, **10**, 2807

www.rsc.org/obc

PAPER

A computational study of the enantioselective addition of n-BuLi to benzaldehyde in the presence of a chiral lithium N,P amide†

Petra Rönnholm, Jürgen Gräfenstein, Per-Ola Norrby, Göran Hilmersson and Sten O. Nilsson Lill*

Received 12th November 2011, Accepted 2nd February 2012
DOI: 10.1039/c2ob06910e

In the presence of a chiral lithium N,P amide, alkylation of benzaldehyde results in an enantioselective formation of 1-phenyl-pentanol. This stereoselective addition reaction has herein been studied using dispersion-corrected density functional theory. For five different chiral ligands originating from amino acids the resulting enantioselectivity has been computationally determined and compared with experimentally available enantiomeric ratios (e.r.). In all cases the experimentally preferred enantiomer could be reproduced by the computational model. The selectivity trend among the ligands was found strongly sensitive to the amount of dispersion correction included. The origin of selectivity in the alkylation reaction is found to be composed of many combined interactions. For the most selective ligand **2A** the most important factors found, which are favouring the (*R*)-TS, are a CH–π interaction between benzaldehyde–dimethyl ether (DME), stronger Li-solvation, and Li–π interactions with the phenyl ring in the backbone of the chiral lithium N,P amide. In addition, solvation by the bulk solvent and the size of the substituent on the nitrogen are also found important factors for the enantioselectivity.

Introduction

Alkyllithium compounds are widely used in organic synthesis because of their strong Brønsted basicity and nucleophilicity, which can be employed to generate new C–C bonds.[1,2] A few examples have been reported regarding the use of alkyllithium reagents in stereoselective C–C bond formations, for example alkylation of imines,[3,4] ketones,[5–8] or aldehydes.[7–21] Other stereoselective reactions involving chiral organolithium compounds are exemplified by: the use of oxiranyllithiums to give substituted epoxides,[22] lithium enolate addition to aldehydes,[23–25] or, using chiral lithium amides rather than alkyllithiums, enantioselective deprotonation reactions.[26–39] One of the potential applications of chiral lithium organic compounds is the synthesis of enantiomerically pure alcohols, which are used for example as intermediates in drug design. During several years, we have systematically studied a model reaction for such a synthesis, *viz.* the enantioselective formation of 1-phenyl-pentanol by nucleophilic 1,2-addition of n-butyllithium (n-BuLi) to benzaldehyde using chiral lithium amides as ligands (Scheme 1). The overall goal has been to design and synthesize chiral ligands that provide both a high yield and, above all, high enantioselectivity. The first ligands investigated by us were lithium amides containing a chelating ether group (N,O ligands).[40] Later on, it was found that N,S ligands, *i.e.* compounds containing a chelating thioether group, surpassed their N,O counterparts with respect to yield and enantioselectivity.[41–43] This finding suggested that the analogous N,P amides could be promising chiral ligands for obtaining even

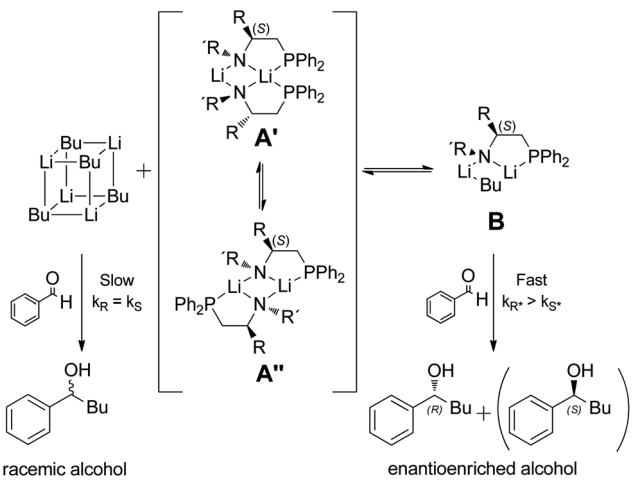

Scheme 1 Formation of 1-phenyl-pentanol by nucleophilic addition of n-BuLi to benzaldehyde with and without chiral lithium amide ligands. R′ = i-Pr, Me; R = i-Pr, Ph, Bn.

Department of Chemistry and Molecular Biology, University of Gothenburg, SE-412 96, Göteborg, Sweden. E-mail: stenil@chem.gu.se; Tel: +46-31-786 9103

†Electronic supplementary information (ESI) available: Figure of constrained bonds in initial geometry optimization. Cartesian coordinates, potential energies, free energies, solvation energies, and dispersion correction energies for the different TSs. See DOI: 10.1039/c2ob06910e

higher enantioselectivities. In order to investigate the hypothesis, an approach to prepare chiral N,P ligands was recently developed.[44]

These ligands were then applied in the n-BuLi addition to benzaldehyde where enantiomeric ratio (e.r.) values in the range between 10 and 99 were obtained. This finding confirmed the potential of chiral lithium N,P amides for stereoselective synthesis.[45] At the same time, the variance in the observed enantioselectivity raised the question how the structure of the ligands affects the stereoselectivity. This question was the starting point for the present computational study where we investigate the transition states (TSs) based on the N,P ligands and the resulting enantioselectivities for the addition reaction.

Due to their high polarity, lithium organic compounds are prone to be aggregated and solvated.[22,46–60] n-BuLi, for example, forms tetramers (see Scheme 1) in non-polar solvents, and solvated dimers in strongly coordinating ethers.[61,62] Similarly, lithium N,P amides form different types of solvated dimers (**A′** or **A″**) as has recently been studied in detail both experimentally and computationally.[45,63] The background reaction, originating from alkylation of the substrate by n-BuLi itself, normally has a relatively high activation barrier due to the stability of the $(n\text{-BuLi})_4$ aggregate, making the ligand-free reaction path relatively slow at −116 °C. Addition of a chiral lithium ligand, for example **A**, deaggregates the homocomplex of n-BuLi forming a chiral heterocomplex **B** which provides the alkylating reagent in a less aggregated and thus more reactive state that may react with benzaldehyde (Scheme 1, right part).[12–16,20,21,41,43,45,64,65] As a result, the ligand-mediated reaction path is faster and dominates the addition reaction over the background reaction. Since the heterocomplex inherits the chirality of chiral amide **A**, the addition reaction is stereospecific and one of the enantiomers of the alcohol is generated in excess. The enantiomeric ratio of products is determined by the difference in the activation barriers for formation of the two alcohol enantiomers, *i.e.* eventually the difference in free energy between the (*S*)- and (*R*)-transition states (TSs), according to the Curtin–Hammett principle.[66–68] Calculating the e.r. for the alcohol formation thus appears rather straightforward. However, one of the main challenges is that the ligands show considerable conformational flexibility generated both by the substituents R, R′ and the phenyl groups in the phosphine moiety.[63] Consequently, there is a large variety of possible TS conformers for each ligand that needs to be systematically analysed to identify the relevant most stable TS for each enantiomer.

In the present work, the enantioselective addition of n-BuLi to benzaldehyde mediated by the chiral ligands **1A–5A** (Fig. 1) has been studied computationally using density functional theory (DFT). For each ligand, all plausible (*S*)- and (*R*)-TSs have been located and the e.r. in the alcohol formation has been determined utilizing dispersion-corrected free energies in solution calculated from the most stable diastereoisomeric TSs. The results are compared to the experimental e.r.-values[44] and the selectivity is rationalized from the TSs. Earlier computational and experimental studies on the alkylation of benzaldehyde in the presence of chiral ligands have been reported,[7,8,10–16,18,20,40,41,43,44,57,69–71] but this appears to be the first computational study utilizing chiral N,P ligands for the title reaction. Interestingly, the first protocol using catalytic amounts of the chiral ligand in enantioselective alkylation of aldehydes was recently published by Maddaluno's group.[21]

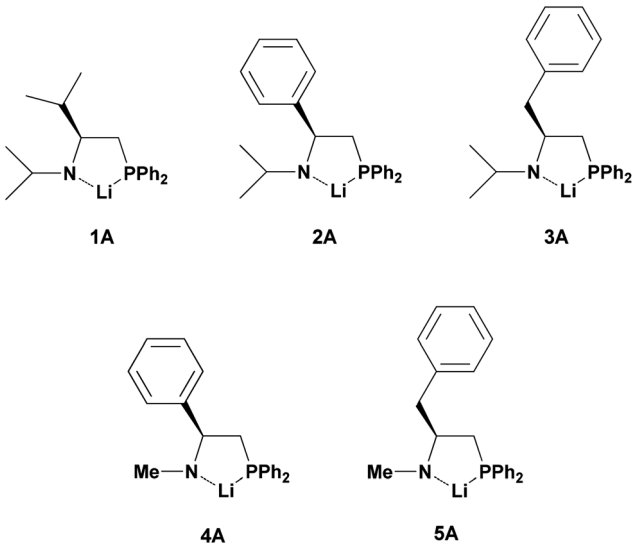

Fig. 1 Putative monomers of chiral lithium N,P-amides investigated in this study.

Methods

All geometries were optimized at the B3LYP/6-31G** level of theory.[72–75] Vibrational frequencies were calculated at the same level of theory to characterize the stationary points, and to determine thermochemical corrections. Solvation energies for the optimized geometries were calculated at the B3LYP/6-31+G** level[76] using the SM8 solvation model with THF as solvent. Grimme's DFT-D3 approach[77] was used to account for dispersion interactions. In a previous DFT-study on lithium amide aggregates we found it necessary to reduce the effect of the dispersion correction to 20% in order to reproduce the experimental observations.[63] However, in that study we focused on to what degree the lithium amide were solvated, by one or two solvent molecules. It has recently been debated that dispersion corrections work very well in the gas-phase or when comparing systems with the same molecularity, for example regioisomers or diastereoisomers, while for example ligand dissociation in solution is less well described and a robust computational protocol to accomplish this has not yet settled. Since we in this study are dealing with diastereoisomeric TSs, we initially wanted to calculate the total energies including either 20% or 100% of the DFT-D3 dispersion energy. The efficiency of the TS geometry optimizations depends largely on a good initial geometry guess. To enhance the throughput of the TS calculations we initially constructed a template for one TS in the following way: Starting from the equilibrium geometry of a DME-solvated heterocomplex **B** for one of the ligands, we replaced the butyl group with an ethyl group, and the two substituents R and R′ were set to methyl groups. The resulting scaffold was merged with a benzaldehyde molecule and a TS search was performed for the complex. The TS found for this model system was then used as a template to locate the TS for the full ligands **1A–5A** and with

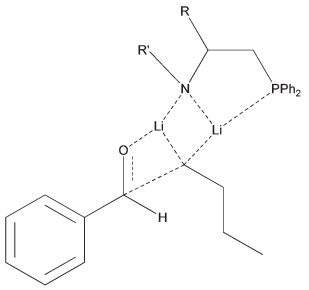

Fig. 2 Schematic picture of the TS in the ligand-mediated addition of n-BuLi to benzaldehyde. R = Ph, Bn, i-Pr and R′ = Me, i-Pr.

n-BuLi, both for (*S*)- and (*R*)-TSs. In the experiments, one of the ligands (**2A**) was chosen so that the (*S*)-product was formed in excess whereas all the others yielded the (*R*)-product. In order to have a uniform basis for the discussion throughout the present computational study, the absolute configuration of **2A** was inverted compared to the experiment. Due to the conformational flexibility of the ligands, a large number of TS searches are required to find the most stable TS for each of them. To additionally save computational resources, the optimizations were performed in two steps: First, all heterocomplexes **B** were optimized using a local version of the MM3* force field.[78] For each ligand, benzaldehyde was merged to all MM3* heterocomplexes within an energy range of 8 kJ mol^{-1} and these were then optimized with DFT. Owing to the complex nature of the reaction coordinate involved in the addition reaction, an initial energy minimization using DFT where some bonds were constrained was performed followed by optimizing to a TS with the constraints lifted. The constrained bonds are depicted in Fig. S1 in the ESI.† To ensure that the investigated TS indeed are describing the reaction of interest an intrinsic reaction path (IRC)[79] analysis was performed for one of the TS which verified that it indeed connects the correct reactants with the correct products. In the explicit solvation of lithium, dimethyl ether (DME) was used as a model for THF or DEE. All DFT calculations were performed with Jaguar[80] and all force-field calculations with MM3* using MacroModel.[81]

Results and discussion

Benzaldehyde coordination

The calculations of the TSs show that the amide nitrogen, the two lithium atoms and the α-carbon of n-BuLi form a central slightly puckered four-membered (N–Li–C–Li) ring which is a common structural pattern in lithium organic chemistry. One of the lithiums is internally coordinated by the phosphorus, while the other lithium coordinates to the carbonyl oxygen of the aldehyde (Fig. 2). A similar coordination motif was found in a PM3 study on the benzaldehyde alkylation reaction.[40]

The TS appears to be early on the reaction coordinate going from the reactant to product as judged by the rather long distance for the C–C bond formed, see below. This result is, according to Hammond's postulate, expected in an exergonic reaction.[14] When analyzing all the generated TSs the first observation made from the optimized structures is that the benzaldehyde

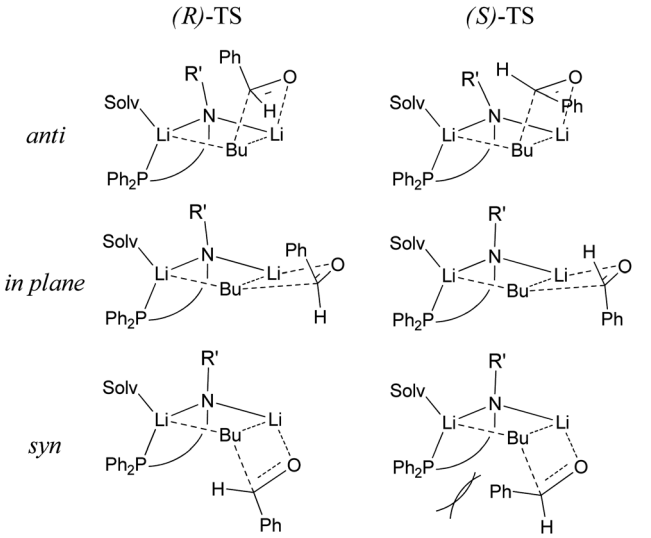

Fig. 3 Schematic representation of the different coordination modes of benzaldehyde in the TSs. Bu = *n*-butyl.

coordination modes can be categorized into three different groups. We will here adopt the nomenclature *syn*, *anti* or *in plane* for this purpose, defined as the relationship between benzaldehyde and the chelating phosphorus with respect to the 4-membered N–Li–C–Li ring (Fig. 3). A similar nomenclature was instructive for stereoselective alkylation reactions using zinc alkyl reagents.[82]

For all ligands it is observed that by far the most frequently occurring coordination mode in the (*S*)-TSs is the *anti*-conformation, although for ligands **3A** and **5A** a few (*S*)-TSs feature the *in plane* conformation. The common characteristic of these two ligands is that both are based on the same phenylalanine amino acid backbone which obviously affects the possible conformation modes. However, it is always found that the *in plane* conformation is less stable than the *anti*-conformation. No *syn*-conformations for the (*S*)-TSs are observed due to a severe steric repulsion between the PPh_2 moiety and the phenyl ring of the benzaldehyde, as depicted in Fig. 3. All (*R*)-TSs for ligand **3A** are in an *anti*-conformation, and also most of the (*R*)-TSs for the other ligands although for these some TSs have benzaldehyde coordinating in the less stable *in plane* conformation.

An important deviator among the ligands is **5A** where it is found that in some (*R*)-TSs the benzaldehyde is coordinating in a *syn*-conformation. Most importantly, the most stable TS for ligand **5A** is in fact the (*R*)-TS with benzaldehyde in *syn*-conformation (Fig. 4). Thus, there appears to be two energetically available paths (*syn* or *anti*) for the major enantiomer resulting in the (*R*)-product, but only one available path (*anti*) for the less stable enantiomer resulting in the (*S*)-product. Thus, already here we can observe a discrimination of the less favoured product route. These results are summarized in Table 1.

Origin of selectivity

With the most stable TS-structures for each ligand now identified, the interesting point is to see if the computational model used predicts/verifies the experimental results regarding the

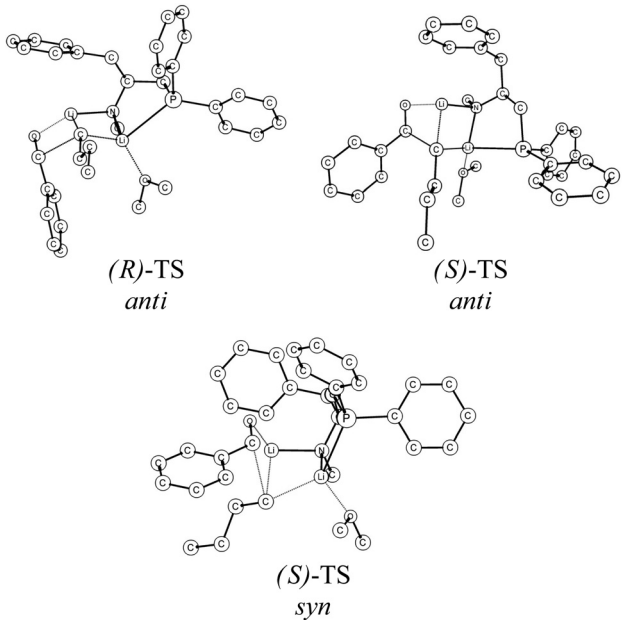

Fig. 4 Different coordination modes for benzaldehyde in (*R*)-TS and (*S*)-TS for ligand **5A**. Hydrogens are omitted for clarity.

Table 1 Observed conformations in the TSs

Ligand	(*R*)-TS	(*S*)-TS
1A	*Anti*	*Anti*
	In-plane	
2A	*Anti*	*Anti*
	In-plane	
3A	*Anti*	*Anti*
		In-plane
4A	*Anti*	*Anti*
	In-plane	
5A	*Syn*	*Anti*
	Anti	*In-plane*
	In-plane	

enantioselectivity. Experimentally, it is found that ligands **1A** and **3A** give a low selectivity (10–30 : 1, Table 2) in the alkylation reaction while ligand **2A** gives a high selectivity (99 : 1). It should be remembered that these selectivities correspond to small relative energies, 3–6 kJ mol^{-1} (see Table 2) making the computational prediction challenging. Gratifyingly, for all ligands the experimentally preferred enantiomer is reproduced by the computational approach. However, the trend of which one of the ligands is the most selective was found more challenging to reproduce. Only when applying Grimme's dispersion correction on top of the solvation free energies could this trend among the different ligands be correctly reproduced.

As pointed out in the Methods section, the total energies were initially calculated either including 0, 20% or 100% of the DFT-D3 dispersion correction term energy (Table 2) to parallel an earlier study on the ground state complexes of the lithium amides.[63] When comparing the results when applying 20% or 100% of the dispersion correction it is indeed observed that inclusion of the full dispersion correction gives a clearly better agreement with the experimental results.[44] The relation between

Table 2 Experimental and calculated enantiomeric ratios at −116 °C with different amounts of dispersion correction included in the final energy. Relative energies (in kJ mol^{-1}) between TSs are given in parentheses

	Calc. enantiomeric ratio with different amount of dispersion correction					
Ligand	0%	20%	65%	100%	100%[c]	Exp.[a]
1A	245 (7.2)	259 (7.3)	295 (7.4)	327 (7.6)	10 (3.0)	28 (4.3)
2A	93 (5.9)	489 (8.1)	20 200 (12.9)	365 000 (16.7)	2 920 000 (19.4)	99 (6.0)
3A	11 500 (12.2)	6400 (11.4)	1723 (9.7)	621 (8.4)	5 (2.1)	10 (3.0)
4A	827 (8.8)	751 (8.6)	605 (8.4)	511 (8.1)	5 (2.1)	—[b]
5A	2900 (10.4)	3640 (10.7)	6020 (11.4)	8920 (11.9)	16 (3.6)	—[b]

[a] Ref. 44. [b] Not determined. [c] Solution phase energies (SM8) removed.

1A and **3A**, with the latter being slightly more selective, could not be correctly reproduced. However, the calculated energy error is only 0.8 kJ mol^{-1}, which is significantly lower than the typical errors found for dispersion-corrected DFT calculated relative energies for diastereoisomeric transition states as shown by a recent benchmark study by Clark and co-workers.[83] An interesting observation is that to achieve the correct ratio (*ca.* 10) in e.r. between ligands **2A** and **3A** a scaling of the dispersion correction close to 65% is needed. This was the scaling of the dispersion effect required found in a previous study.[84] Other studies have also suggested that calculated dispersion effects are slightly overestimated.[85,86] Especially noteworthy are that the dispersion corrections for ligands **2A** and **3A** are opposite. For ligand **2A**, the dispersion correction *increases* the free energy gain for the (*R*)-TS by 11 kJ mol^{-1} while for ligand **3A** the free energy difference is *reduced* by 4 kJ mol^{-1} (see Table 2). For ligands **4A** and **5A**, where the experimental selectivity is yet unknown, we predict that ligand **4A** will give a low selectivity, similarly or lower than that found for **1A** and **3A**, while ligand **5A** is predicted to have the second highest selectivity among the five ligands investigated in this study. Overall, the calculated enantioselectivity is overestimated for ligands **1A–3A** compared to the experimentally observed selectivities. This is a rather general phenomenon observed when calculating enantioselectivities,[87] and may have its origin from overestimation of the entropy term due to the neglect of anharmonicity or the fact that the geometry optimizations were performed in the gas-phase rather than in the solution phase. Another important factor to bear in mind is that experimentally any background reaction will lower the enantiomeric ratio, while computationally the "pure" reactions are always considered. The large computational energy difference between TSs for ligand **2A** (19 kJ mol^{-1}) compared to the experimental value (6 kJ mol^{-1}) may indicate that in this system we have a higher degree of a competitive background reaction compared to the other ligands, *i.e.* the ligand is kinetically slow but highly enantioselective. Interestingly, Friesner and co-workers have suggested an overall scaling factor (2/3) before using free energies to calculate the enantiomeric ratios.[87] If that procedure is applied to the present study, and then adding the full

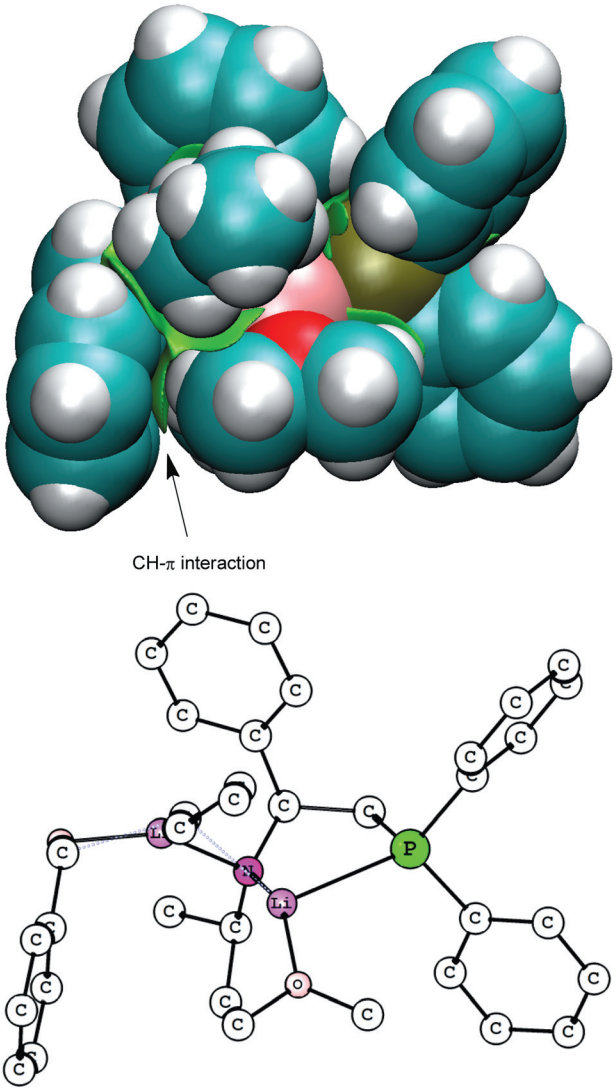

Fig. 5 (a) NCI-plot visualizing the dispersion effects (green) in the (*R*)-TS for ligand **2A**. (b) The structure of the TS with the view set as in (a) for comparison, and with hydrogens removed.

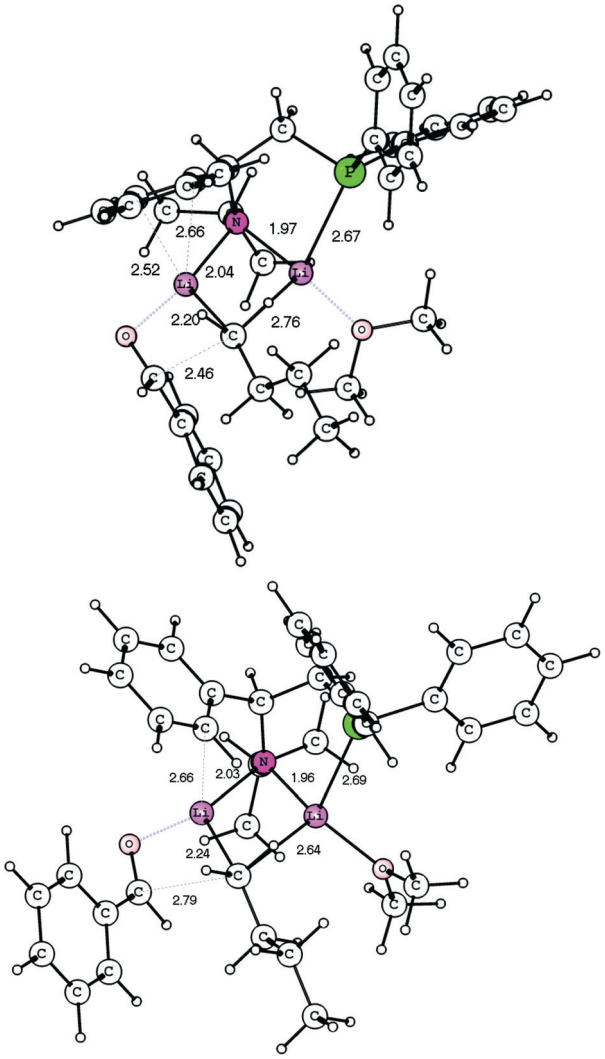

Fig. 6 Geometry optimized structure of (*R*)-TS (top) and (*S*)-TS (bottom) for ligand **2A**.

dispersion correction the correct selectivity order between ligands **1A** and **3A** is achieved (e.r. = 55 and 29, respectively) while ligand **2A** is still the most selective (e.r. = 71 400).

The reason for the large dispersion effects favouring (*R*)-TS for ligand **2A** was investigated using two different approaches: (a) non-covalent interaction (NCI) plots,[88] a recently introduced tool to visualize for example dispersion interactions or hydrogen bonds[84,89] and (b) calculation of Grimme's dispersion effects for different fragments of the TSs. Interestingly, the clearly largest difference in dispersion effect between (*R*)- and (*S*)-TS originates from the interaction between the phenyl ring of benzaldehyde and one hydrogen in the solvent DME (as pointed out in Fig. 5). This interaction is only found in (*R*)-TS since in the other, diastereoisomeric, TS the phenyl ring is distanced from the coordinating solvent molecule by *ca.* 7 Å (Fig. 6). The stabilizing interaction between the slightly positive α-proton of DME and the phenyl ring is nicely visualized by a NCI plot (Fig. 5).[88] The present study appears to be the second in the literature taking advantage of NCI as a tool in understanding enantioselectivities. Jacobsen and co-workers used the same approach in studying enantioselective protonation of enol silanes using chiral sulfinamides.[90]

The benzaldehyde–DME effect stabilizing (*R*)- over (*S*)-TS seems to be dependent on the R′-substituent on the nitrogen in the ligand since for ligands **4A** and **5A** with R′ = Me this effect is found to be opposite. This is likely an effect of the more bulky i-Pr group in ligands **1A–3A** (*A*-value 2.15 *vs.* 1.7 for Me) which may interact with both the phenyl ring in benzaldehyde and the solvent DME and thus assists directing the solvent. It has previously been argued that a bulky substituent on the nitrogen (R′) is the most important factor responsible for a high selectivity,[17,40] and this can now partially be understood. However, by comparing ligands **1A–3A** which all have the same R′-group (i-Pr) we see that the selectivity is also strongly dependent on the R-group at the backbone of the ligand. Thus, the origin of the selectivity is much more complex than one first may anticipate. In addition to the substrate–solvent interaction described above, the phenyl ring in the backbone of the ligand **2A** forms a

Table 3 Rank, based on difference in dispersion interaction energies, favouring (*R*)-TS[a]

Ligand	a–b	a–c	a–d	b–c	b–d	c–d	d	Total rank
1A	4	**2**	**2**	3	2	2	3	18
2A	2	**1**	**3**	4	**1**	1	1	13
3A	3	3	4	2	3	4	4	23
5A	1	4	**1**	1	4	3	2	16

[a] Interactions >5 kJ mol^{-1} favouring (*R*)-TS are highlighted in bold.

η^2-coordination to one of the lithiums in the N–Li–C–Li ring in (*R*)-TS, while in (*S*)-TS this coordination is reduced to only a η^1-coordination (Fig. 6). The energy difference contribution originating from dispersion only between these different coordination modes is estimated to be *ca.* 6 kJ mol^{-1}. In addition to this, one should add the electrostatic cation–π interaction between the lithium and the phenyl ring.

These two effects favouring the (*R*)-TS are to some extent counterbalanced by other effects favouring (*S*)-TS, for example between DME and the alkylating group, but are at least important ingredients in the selectivity pot. The impact of Li–π interactions on the enantioselectivity has been discussed before,[16] but it has also been suggested that the R-group can be either an alkyl or an aryl group resulting in similar selectivities.[40] This contradicts the results using the present N,P-ligands where there is a large difference in selectivity when comparing ligands **1A** and **2A**.

Some other general phenomena for all ligands observed are that for the *anti*-TSs the transferred alkyl group shows a larger dispersion interaction with the phenyl ring in benzaldehyde in the (*S*)-TS than in (*R*)-TS, ranging from 0.1 to 4 kJ mol^{-1}. The smallest of these numbers are found for the most selective ligand **2A**, thus here the (*S*)-selectivity giving effect is most strongly reduced. Similarly, the internal dispersion effect in the ligand that is favouring (*R*)-TS is found largest for ligand **2A**.

Since the TS geometries are very complex and many small interactions are counterbalanced it is hard to pinpoint a specific interaction that is the sole reason for the enantioselectivity. An attempt to do this is by simply sketching the TS as built from four units: (a) benzaldehyde (b) n-BuLi (c) Li-DME (d) ligand (compare Fig. 2) and finally rank the different dispersion interactions between the units based on the energy difference between the TSs favouring (*R*)-TS, and then make a comparison between the different ligands. This allows the identification of what interactions are enhanced in the different ligands and thus generates a selectivity modification. Such a comparison is presented in Table 3, where the lowest score for a particular interaction should be interpreted as resulting in the highest selectivity for the (*R*)-TS. Ligand **4A** has been excluded from this analysis since the differences in dispersion effects between TSs were found very small (less than 1 kJ mol^{-1}).

By this simple analysis it is found that ligand **2A** has the lowest rank and thus overall is favouring the (*R*)-TS, while ligand **3A** is clearly the ligand least favouring the (*R*)-TS. This is in accordance with the experimental results and also with the calculated enantiomeric ratios presented in Table 2. We see that ligand **2A** has the lowest rank in four out of the seven interaction criteria used, and shows a strong (*R*)-TS preference (>5 kJ mol^{-1}) in three of the interaction categories: benzaldehyde–LiDME, benzaldehyde–ligand, and n-BuLi–ligand. Thus, the analysis for ligand **3A** identifies that the underlying dispersion effects that help to stabilize (*S*)-TS, and thus reduce the enantioselectivity, are dominated by the interaction between DME and the ligand. In particular we observe the dispersion interaction to the i-Pr group on nitrogen with a H(DME)–H(i-Pr) distance of 2.3 Å, which is smaller than the sum of van der Waals radii of two hydrogens (2.4 Å).

For ligand **5A**, the most stable TS adopts a *syn* conformation which makes the selectivity determining factors a bit different. The *syn* conformation, only available in the (*R*)-TS as discussed above, makes the BuLi–benzaldehyde interaction stronger in (*R*)-TS than in (*S*)-TS as opposed to the other ligands. In addition, the benzaldehyde–ligand interaction strongly favours the (*R*)-TS. Of particular note here is the finding of an interaction between phosphorus and the aldehyde hydrogen, but also between the aldehyde oxygen and one of the hydrogens at the β-carbon of the backbone of the ligand forming a weak hydrogen bond (2.5 Å).

In addition to the differences in dispersion interactions described above, it is found that the Li–solvent interaction is stronger in the (*R*)-TSs than in (*S*)-TSs for ligands **1A–3A** as judged by shorter Li–O distances (*ca.* 0.03–0.07 Å difference). For ligands **4A–5A** the differences are too small (0.01 Å) to be interpretable. In addition to these specific interactions, it is also found that the bulk solvent described by the SM8 solvation model in general stabilizes the (*R*)-TS better than the (*S*)-TS and thus enhances the enantioselectivity (Table 2). The only exception is ligand **3A** where a very high selectivity is reduced by the solvation model but still yields the highest selectivity among all ligands. This finding, together with the fact that the largest dispersion energy differences involves interactions between the benzaldehyde and the solvent fits well with earlier studies, where it has been shown that the enantioselectivity is strongly dependent on the solvent.[9,12,20,40,41,91,92]

Conclusions

A detailed computational investigation of the enantioselective addition of n-BuLi to benzaldehyde in the presence of a chiral lithium N,P-amide is presented. Five different chiral ligands originally synthesized from amino acids were studied using dispersion-corrected DFT, and the resulting enantioselectivity has been compared with experimentally available enantiomeric ratios. Gratifyingly, the experimentally preferred enantiomers were correctly reproduced for all ligands. Different amounts of Grimme's dispersion correction terms were tested in order to reproduce the selectivity trend among ligands. It is found that inclusion of the full dispersion correction gives the best agreement with experimental data. The origin of the enantioselectivity for the most selective ligand was found to include specific interactions between the solvent and the substrate benzaldehyde, stronger Li–solvent interaction, and Li–π interactions to the phenyl ring in the backbone of the chiral lithium N,P amide. The continuum solvation model was in general found to stabilize the preferred diastereoisomeric (*R*)-TS better than the (*S*)-TS and thus elevating the enantioselectivity.

Acknowledgements

The computational studies were performed on resources provided by the Swedish National Infrastructure for Computing (SNIC) at C3SE. S.O.N.L. acknowledges financial support from The Åke Wiberg Foundation.

Notes and references

1 M. Wills, *Contemp. Org. Synth.*, 1996, **3**, 201–228.
2 J. Clayden, *Organolithium: Selectivity for Synthesis*, Pergamon, Oxford, 2002.
3 G. Cainelli, D. Giacomini and M. Walzl, *Angew. Chem., Int. Ed. Engl.*, 1995, **34**, 2150–2152.
4 Nancy, S. Ghosh, N. Singh, N. G. Kaur, P. Venugopalan, P. V. Bharatam and S. Trehan, *Chem. Commun.*, 2003, 1420–1421.
5 K. Ando, K. R. Condroski, K. N. Houk, Y.-D. Wu, S. K. Ly and L. E. Overman, *J. Org. Chem.*, 1998, **63**, 3196–3203.
6 M. Imai, A. Hagihara, H. Kawasaki, K. Manabe and K. Koga, *Tetrahedron*, 1999, **56**, 179–185.
7 B. Goldfuss, *Synthesis*, 2005, 2271–2280.
8 M. R. Luderer, W. F. Bailey, M. R. Luderer, J. D. Fair, R. J. Dancer and M. B. Sommer, *Tetrahedron: Asymmetry*, 2009, **20**, 981–998.
9 T. Mukaiyama, K. Soai, T. Sato, H. Shimizu and K. Suzuki, *J. Am. Chem. Soc.*, 1979, **101**, 1455–1460.
10 L. Colombo, C. Gennari, G. Poli and C. Scolastico, *Tetrahedron*, 1982, **38**, 2725–2727.
11 M. B. Eleveld and H. Hogeveen, *Tetrahedron Lett.*, 1984, **25**, 5187–5190.
12 G. Hilmersson and Ö. Davidsson, *J. Organomet. Chem.*, 1995, **489**, 175–179.
13 L. M. Pratt and I. M. Khan, *Tetrahedron: Asymmetry*, 1995, **6**, 2165–2176.
14 A. Corruble, J.-Y. Valnot, J. Maddaluno, Y. Prigent, D. Davoust and P. Duhamel, *J. Am. Chem. Soc.*, 1997, **119**, 10042–10048.
15 C. Fressigne, A. Corruble, J.-Y. Valnot, J. Maddaluno and C. Giessner-Prettre, *J. Organomet. Chem.*, 1997, **549**, 81–88.
16 P. I. Arvidsson, Ö. Davidsson and G. Hilmersson, *Tetrahedron: Asymmetry*, 1999, **10**, 527–534.
17 P. I. Arvidsson, G. Hilmersson and Ö. Davidsson, *Chem.–Eur. J.*, 1999, **5**, 2348–2355.
18 B. Goldfuss, M. Steigelmann and F. Rominger, *Angew. Chem., Int. Ed.*, 2000, **39**, 4133–4136.
19 R. Sott, J. Granander and G. Hilmersson, *Chem.–Eur. J.*, 2002, **8**, 2081–2087.
20 J. Liu, D. Li, C. Sun and P. G. Williard, *J. Org. Chem.*, 2008, **73**, 4045–4052.
21 B. Lecachey, C. Fressigne, H. Oulyadi, A. Harrison-Marchand and J. Maddaluno, *Chem. Commun.*, 2011, **47**, 9915–9917.
22 V. Capriati, S. Florio, F. M. Perna, A. Salomone, A. Abbotto, M. Amedjkouh and S. O. Nilsson Lill, *Chem.–Eur. J.*, 2009, **15**, 7958–7979.
23 M. Muraoka, H. Kawasaki and K. Koga, *Tetrahedron Lett.*, 1988, **29**, 337–338.
24 M. Majewski and D. M. Gleave, *J. Org. Chem.*, 1992, **57**, 3599–3605.
25 D. Hoppe and T. Hense, *Angew. Chem., Int. Ed. Engl.*, 1997, **36**, 2282–2316.
26 P. J. Cox and N. S. Simpkins, *Tetrahedron: Asymmetry*, 1991, **2**, 1–26.
27 K. Koga, *Pure Appl. Chem.*, 1994, **66**, 1487–1492.
28 N. S. Simpkins, *Pure Appl. Chem.*, 1996, **68**, 691–694.
29 S. Wu, S. Lee and P. Beak, *J. Am. Chem. Soc.*, 1996, **118**, 715–721.
30 V. K. Aggarwal, P. S. Humphries and A. Fenwick, *J. Chem. Soc., Perkin Trans. 1*, 1999, 2883–2889.
31 E.-U. Würthwein, K. Behrens and D. Hoppe, *Chem.–Eur. J.*, 1999, **5**, 3459–3463.
32 W. F. Bailey, P. Beak, S. T. Kerrick, S. Ma and K. B. Wiberg, *J. Am. Chem. Soc.*, 2002, **124**, 1889–1896.
33 M. Hansson, P. I. Arvidsson, S. O. Nilsson Lill and P. Ahlberg, *J. Chem. Soc., Perkin Trans. 2*, 2002, 763–767.
34 P. O'Brien and C. D. Pilgram, *Org. Biomol. Chem.*, 2003, **1**, 523–534.
35 L. M. Pratt, A. Newman, J. St. Cyr, H. Johnson, B. Miles, A. Lattier, E. Austin, S. Henderson, B. Hershey, M. Lin, Y. Balamraju, L. Sammonds, J. Cheramie, J. Karnes, E. Hymel, B. Woodford and C. Carter, *J. Org. Chem.*, 2003, **68**, 6387–6391.
36 P. Brandt, P.-O. Norrby and P. G. Andersson, *Tetrahedron*, 2003, **59**, 9695–9700.
37 S. O. Nilsson Lill, P. Dinér, D. Pettersen, M. Amedjkouh and P. Ahlberg, in *Adv. Quantum Chem.*, ed. E. Brandas, Academic Press, 2004, vol. 47, pp. 1–22.
38 P. Dinér, D. Pettersen, S. O. Nilsson Lill and P. Ahlberg, *Tetrahedron: Asymmetry*, 2005, **16**, 2665–2671.
39 D. Pettersen, M. Amedjkouh and P. Ahlberg, *The Chemistry of Organolithium Compounds* John Wiley & Sons, Ltd, 2006, pp. 411–476.
40 J. Granander, R. Sott and G. Hilmersson, *Tetrahedron*, 2002, **58**, 4717–4725.
41 J. Granander, R. Sott and G. Hilmersson, *Tetrahedron: Asymmetry*, 2003, **14**, 439–447.
42 R. Sott, J. Granander, P. Dinér and G. Hilmersson, *Tetrahedron: Asymmetry*, 2004, **15**, 267–274.
43 J. Granander, J. Eriksson and G. Hilmersson, *Tetrahedron: Asymmetry*, 2006, **17**, 2021–2027.
44 P. Rönnholm, M. Södergren and G. Hilmersson, *Org. Lett.*, 2007, **9**, 3781–3783.
45 P. Rönnholm and G. Hilmersson, *ARKIVOC*, 2011, **2011**, 200–210.
46 D. R. Armstrong, D. Barr, R. Snaith, W. Clegg, R. E. Mulvey, K. Wade and D. Reed, *J. Chem. Soc., Dalton Trans.*, 1987, 1071–1081.
47 A. B. Sannigrahi, T. Kar, B. G. Niyogi, P. Hobza and P. v. R. Schleyer, *Chem. Rev.*, 1990, **90**, 1061–1076.
48 W. Bauer, in *Lithium Chemistry: A Theoretical and Experimental Overview*, ed. A.-M. Sapse and P. v. R. Schleyer, John Wiley & Sons, Inc., New York, 1995, p. 595.
49 A.-M. Sapse and P. v. R. Schleyer, *Lithium Chemistry: A Theoretical and Experimental Overview*, John Wiley & Sons, Inc., New York, 1995.
50 A. Streitwieser, S. M. Bachrach, A. E. Dorigo and P. v. R. Schleyer, in *Lithium Chemistry: A Theoretical and Experimental Overview*, ed. A.-M. Sapse and P. v. R. Schleyer, John Wiley & Sons, New York, 1995.
51 S. O. Nilsson Lill, P. I. Arvidsson and P. Ahlberg, *Acta Chem. Scand.*, 1998, **52**, 280–284.
52 H. J. Reich, D. P. Green, M. A. Medina, W. S. Goldenberg, B. Ö. Gudmundsson, R. R. Dykstra and N. H. Phillips, *J. Am. Chem. Soc.*, 1998, **120**, 7201–7210.
53 G. L. J. Van Vliet, F. J. J. De Kanter, M. Schakel, G. W. Klumpp, A. L. Spek and M. Lutz, *Chem.–Eur. J.*, 1999, **5**, 1091–1094.
54 P. I. Arvidsson and Ö. Davidsson, *Angew. Chem., Int. Ed.*, 2000, **39**, 1467–1469.
55 G. Hilmersson, *Chem.–Eur. J.*, 2000, **6**, 3069–3075.
56 X. F. Sun, M. D. Winemiller, B. S. Xiang and D. B. Collum, *J. Am. Chem. Soc.*, 2001, **123**, 8039–8046.
57 A. Corruble, D. Davoust, S. Desjardins, C. Fressigne, C. Giessner-Prettre, A. Harrison-Marchand, H. Houte, M. C. Lasne, J. Maddaluno, H. Oulyadi and J. Y. Valnot, *J. Am. Chem. Soc.*, 2002, **124**, 15267–15279.
58 S. T. Liddle and W. Clegg, *J. Chem. Soc., Dalton Trans.*, 2002, 3923–3924.
59 S. O. Nilsson Lill, U. Köhn and E. Anders, *Eur. J. Org. Chem.*, 2004, 2868–2880.
60 S. O. Nilsson Lill, *THEOCHEM*, 2008, **866**, 81–81.
61 J. F. McGarrity, C. A. Ogle, Z. Brich and H. R. Loosli, *J. Am. Chem. Soc.*, 1985, **107**, 1810–1815.
62 I. Keresztes and P. G. Williard, *J. Am. Chem. Soc.*, 2000, **122**, 10228–10229.
63 P. Rönnholm, S. O. Nilsson Lill, J. Gräfenstein, P.-O. Norrby, M. Pettersson and G. Hilmersson, *Submitted for publication*, 2012.
64 P. G. Williard and C. Sun, *J. Am. Chem. Soc.*, 1997, **119**, 11693–11694.
65 G. Hilmersson and B. Malmros, *Chem.–Eur. J.*, 2001, **7**, 337–341.
66 D. Y. Curtin, *Rec. Chem. Prog.*, 1954, **15**, 111–128.
67 L. P. Hammett, *Physical Organic Chemistry; Reaction Rates, Equilibria, and Mechanisms (McGraw-Hill Series in Advanced Chemistry)*, McGraw-Hill, 2nd edn, 1970.
68 N. S. Zefirov, *Tetrahedron*, 1977, **33**, 2719–2722.
69 E. Kaufmann, P. v. R. Schleyer, K. N. Houk and Y. D. Wu, *J. Am. Chem. Soc.*, 1985, **107**, 5560–5562.
70 C. Fressigne, J. Maddaluno, A. Marquez and C. Giessner-Prettre, *J. Org. Chem.*, 2000, **65**, 8899–8907.
71 B. Goldfuss, M. Steigelmann, F. Rominger and H. Urtel, *Chem.–Eur. J.*, 2001, **7**, 4456–4464.
72 A. D. Becke, *J. Chem. Phys.*, 1993, **98**, 5648–5652.

73 C. Lee, W. Yang and R. G. Parr, *Phys. Rev. B*, 1988, **37**, 785–789.
74 P. J. Stephens, F. J. Devlin, C. F. Chabalowski and M. J. Frisch, *J. Phys. Chem.*, 1994, **98**, 11623–11627.
75 P. C. Hariharan and J. A. Pople, *Theor. Chim. Acta*, 1973, **28**, 213–222.
76 T. Clark, J. Chandrasekhar, G. W. Spitznagel and P. v. R. Schleyer, *J. Comput. Chem.*, 1983, **4**, 294–301.
77 S. Grimme, J. Antony, S. Ehrlich and H. Krieg, *J. Chem. Phys.*, 2010, **132**, 154104.
78 P. Rönnholm and S. O. Nilsson Lill, *Manuscript in preparation*, 2012.
79 K. Fukui, *Acc. Chem. Res.*, 1981, **14**, 363–368.
80 Jaguar, version 7.6, release 211, Schrodinger, LLC, New York, NY, 2010.
81 MacroModel,Schrödinger Inc., New York, NY, 2010, www.schrodinger.com
82 T. Rasmussen and P.-O. Norrby, *J. Am. Chem. Soc.*, 2003, **125**, 5130–5138.
83 S. Schenker, C. Schneider, S. B. Tsogoeva and T. Clark, *J. Chem. Theory Comput.*, 2011, **7**, 3586–3595.
84 S. O. Nilsson Lill, *Phys. Chem. Chem. Phys.*, 2011, **13**, 16022–16027.
85 V. Barone, M. Biczysko and M. Pavone, *Chem. Phys.*, 2008, **346**, 247–256.
86 L. A. Burns, A. V. Mayagoitia, B. G. Sumpter and C. D. Sherrill, *J. Chem. Phys.*, 2011, **134**, 084107–084125.
87 S. T. Schneebeli, M. L. Hall, R. Breslow and R. Friesner, *J. Am. Chem. Soc.*, 2009, **131**, 3965–3973.
88 J. Contreras-Garcia, E. R. Johnson, S. Keinan, R. Chaudret, J.-P. Piquemal, D. N. Beratan and W. Yang, *J. Chem. Theory Comput.*, 2011, **7**, 625–632.
89 S. O. Nilsson Lill, P. Ryberg, T. Rein, E. Bennström and P. O. Norrby, *Chem.–Eur. J.*, 2012, **18**, 1640–1649.
90 E. M. Beck, A. M. Hyde and E. N. Jacobsen, *Org. Lett.*, 2011, **13**, 4260–4263.
91 M. Ye, S. Logaraj, L. M. Jackman, K. Hillegass, K. A. Hirsh, A. M. Bollinger, A. L. Grosz and V. Mani, *Tetrahedron*, 1994, **50**, 6109–6116.
92 A. Abbotto, S. S.-W. Leung, A. Streitwieser and K. V. Kilway, *J. Am. Chem. Soc.*, 1998, **120**, 10807–10813.

